Hindawi
Advances in Civil Engineering
Volume 2020, Article ID 8897777, 8 pages
https://doi.org/10.1155/2020/8897777

Research Article

Lower Bound Solution of Foundation Bearing Capacity beneath Strip Footing Based on Parabolic Mohr Failure Criterion

Fang Wei [1] and Shi Li-jun [2]

[1]School of Traffic and Transportation Engineering, Changsha University of Science & Technology, Changsha 410114, China
[2]Hunan Hongshang Testing Technology Co., Ltd., Changsha 410208, China

Correspondence should be addressed to Fang Wei; fangwei5642366@163.com

Received 18 June 2020; Revised 4 September 2020; Accepted 7 September 2020; Published 15 September 2020

Academic Editor: Xinyu Ye

The static allowable stress field of foundation under strip foundation is constructed by means of stress columns, and the calculation method of the lower bound foundation bearing capacity based on the two-parameter parabolic Mohr yield criterion is proposed. Moreover, the influence of the amount of stress columns and material mechanical parameters on the lower bound bearing capacity is analyzed. The results show that a better solution can be obtained by optimizing the static allowable stress field. However, the improvement of lower bound solution might be inefficient if the stress column amount is large enough. The stresses of the superimposition area show a reduction with the improvement of stress field; on the other hand, the superposed stresses are enhanced ever faster as the involved stress column increases. The tensile-compressive strength ratio has a moderate effect on the lower bound solution. Finally, the reliability of the proposed method is verified by some rock foundation loading tests.

1. Introduction

In the mid-20th century, Drucker and Prager combined the static field and the kinematical field and put forward the limit analysis theory including upper and lower bound analysis, which provided a new tool for solving bearing capacity of foundations. In comparison, the lower limit method is not so widely used because it is more difficult to establish a static allowable stress field. Up to now, the lower bound limit method is mainly composed of two implementation means. Firstly, the construction of static permissible stress field is carried out by superposing stress fields or specifying stress discontinuities [1]. Secondly, the finite element method and mathematical programming tools are employed to acquire the limit state of engineering structures in discrete stress field [2]. In order to get the lower bound solution of bearing capacity for strip footings, Chen adopted the first method and presented the analytical solution subject to linear Mohr-Coulomb criterion [1]. Subsequently, Andrei obtained the lower bound of bearing capacity of weightless foundation beneath strip footing by using limit analysis finite element method [3] and compared the solving efficiency of linear and nonlinear programming. By means of finite element method and linear programming, Li and Liu [4] constructed a static allowable stress field to calculate the slope bearing capacity. Theoretically, the lower bound bearing capacity of the strip footing can be obtained by considering the slope angle to be zero. Zhang et al. derived the lower bound solution of the bearing capacity of the strip footing under compound loading mode [5]. However, the linear yield criterion used in the above literature is quite distant from the actual behaviors of geotechnical materials. How to perform the lower bound analysis accompanied by the nonlinear failure criterion to explore the ultimate bearing capacity of strip footing remains an important subject to be solved.

In 1965, Murrell pointed out that there was a power function relationship between the large and small principal stresses of rocks [6]. Mello also suggested a power function relationship between the shear strength and normal stress of rockfill in 1977 [7], and Perry analyzed slope stability by adopting power function shear strength envelope in 1994

[8]. Besides, Duncan et al. proposed the logarithmic relationship between the friction angle, atmospheric pressure, and small principal stress in coarse-grained soil, which was adopted by "design specification for rolled earth-rock fill dams (SL274-2001)" of China [9, 10]. In 1987, the generalized nonlinear strength criterion was employed in the finite element calculation of safety factor of geotechnical structures [11, 12]. Additionally, some researchers compared the characteristics and applicability of linear criterion, parabolic criterion, hyperbolic criterion, and exponential strength criterion [13–16]. The research shows that each nonlinear strength criterion has advantages and disadvantages in variant application fields, but all of them are more practical than the linear strength criterion.

In this paper, the parabolic yield criterion with two parameters is investigated based on the nonlinear strength theory and the principle pf "simple expression form, explicit physical meaning, and easy parameter obtainment." Subsequently, the static allowable stress field conforming to the lower bound theory is constructed by using multiple stress columns in the spatial foundation beneath strip footing. Finally, the lower bound solution of bearing capacity is obtained with the consideration of the nonlinear parabolic strength criterion.

2. Theoretical Background

2.1. The Lower Bound Theorem. Foundation bearing capacity, Earth pressure, and slope stability are regarded as three classical problems of soil mechanics [17–19]. Figure 1(a) displays a typical load-deformation curve of loading tests on surficial footings. The curve contains four sections, which successively represent elastic, elastoplastic, and plastic deformation and strain hardening stage. In order to determine the ultimate bearing capacity (P_c) of the foundation as an elastoplastic material, two methods are usually adopted: one is to investigate the whole evolution process of the foundation, from elastic deformation state to plastic limit state, which is based on the theory of plastoelasticity mechanics (Figure 1(b)). Due to the complexity of practical engineering problems, it is usually only suitable for simple working conditions. The second is to ignore the process of elastic deformation, regard the material as a rigid-plastic body, and focus on the behavior of the structure in the plastic limit state, namely, the limit analysis method (Figure 1(c)). It can effectively simplify the analysis process and reflect the most essential content in the plastic deformation, so it is widely used in the engineering field.

If there exists a static allowable stress field throughout the whole object without any yield, which can balance with the load acting on the stress boundary, the object will never fail. When the deformation of the object reaches the limit state, the power of the real surface force in the given velocity field is always greater than (or equal to) the power of the corresponding surface force in the same velocity field of any other static allowable field. The lower bound theorem indicates that (1) the ideal object can adjust itself to take on the potential external load; (2) among all the loads corresponding to the static allowable stress field, the ultimate load is the largest.

In general, the lower bound theorem can be cooperated with the upper bound theorem to define the actual interval of the ultimate load. If the upper limit is equivalent to the lower limit, then the ultimate load is a complete solution.

2.2. Two-Parameter Parabolic Mohr Strength Criterion. In 1979, the two-parameter parabolic Mohr strength criterion (as shown in Figure 2) was carried out based on tensile/compressive strength of materials [20]: where σ and τ represent the normal and shear stress, respectively; λ is the intermediate parameter, while σ_c and σ_t are the uniaxial compressive and tensile strength. The proposed criterion is of concise form, clear meaning, and easy accession of parameters. Furthermore, it owns the following properties: (1) the $\sigma\sim\tau$ curve is orthogonal to the σ-axis, which ensures that the curve also has physical significance in the vicinity area of $\tau = 0$; (2) the dip angle of the $\sigma\sim\tau$ curve decreases infinitely with the increasing of σ, conforming with nonlinear Mohr-Coulomb criterion; (3) the two-parameter parabolic Mohr strength criterion is applicable to self-consistently describe compression-shear failure and tension-shear failure, as well as pure tension yielding [21].

$$\begin{cases} \tau^2 = \lambda\left(\sigma + \sigma_t\right), \\ \lambda = \sigma_c + 2\sigma_t - 2\sqrt{\sigma_c\sigma_t + {\sigma_t}^2}. \end{cases} \tag{1}$$

Another form of parabolic Mohr criterion was researched which could be stated as [22, 23]

$$\sigma = a\tau^2 + b, \tag{2}$$

where

$$a = \frac{\sigma_c + 2\sigma_t^2 + 2\sqrt{\sigma_c\sigma_t + {\sigma_t}^2}}{{\sigma_c}^2}, \tag{3}$$

$$b = -\sigma_t. \tag{4}$$

From equations (1) and (3),

$$\lambda \cdot a = 1. \tag{5}$$

Conclusively, the above two models are completely equivalent to each other. The two-parameter parabolic Mohr criterion is not only the development of the classic Mohr-Coulomb criterion but also the extension of the Griffith criterion, and it has good application prospects. However, there exists an implicit constraint; that is, $\sigma_c/\sigma_t > 3$ [24].

3. The Stress Field and the Lower Bound Solution of Bearing Capacity

In this research, the following assumptions are adopted: (1) the foundation locates beneath a strip footing with a frictionless bottom; (2) the foundation is weightless; (3) the foundation is a rigid-plastic body, subject to the parabolic Mohr yield criterion.

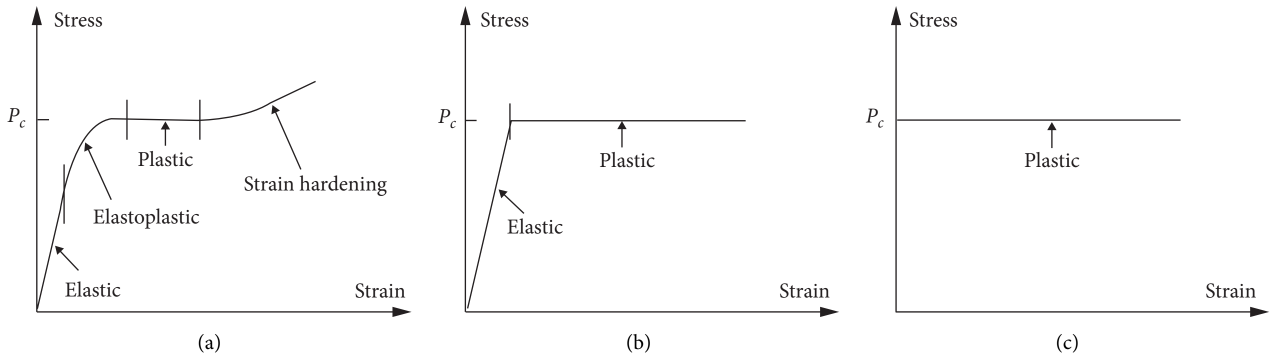

Figure 1: Deformation curves: (a) common material; (b) ideal elastoplasticity; (c) rigid plasticity.

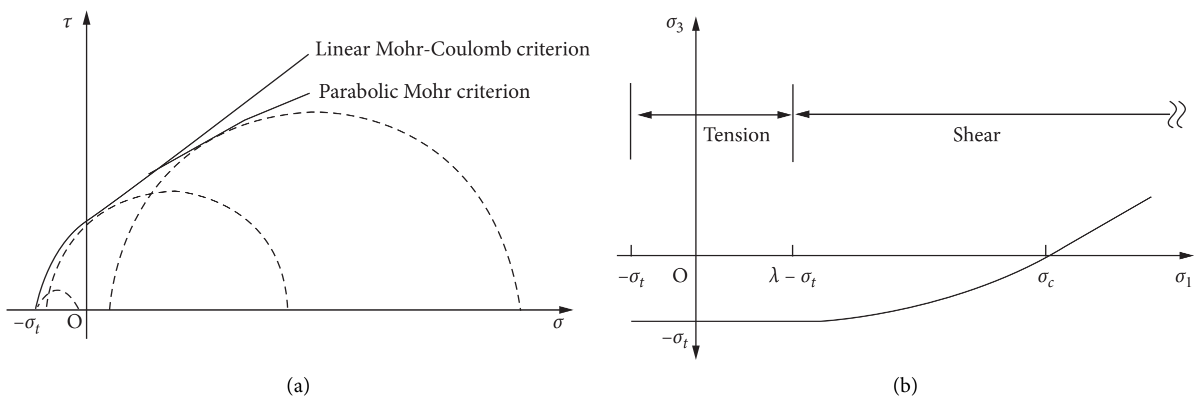

Figure 2: Parabolic Mohr strength criterion in different coordinate systems: (a) $\sigma{\sim}\tau$; (b) $\sigma_1{\sim}\sigma_3$.

3.1. The Case of a Single Stress Column. For the simplest case, only one stress column beneath strip footing is taken into consideration (Figure 3), which could be regarded as uniaxial compression.

Therefore, the lower bound solution of bearing capacity of the foundation (σ_z) could be given by

$$\sigma_z = R = \sigma_c, \tag{6}$$

in which R is the yield strength. However, all experiences show that the stress in the foundation is transmitted by diffusion. Obviously, in the case of one stress column, the material strength on both sides of the stress column is not considered at all.

3.2. The Case of Three Stress Columns. Subsequently, a static allowable spatial stress field is shown in Figure 4, which is constructed by three stress columns: a vertical stress column under strip footing and two lateral stress columns symmetrically arranged on the left and right sides. In Figure 4, Q and α are unknown parameters. In order to ensure that the stress state of any point in the foundation does not violate the yield criterion after the superposition of stress fields, a horizontal stress column is added in the foundation with an axial compression of $R = \sigma_c$.

According to [20], the two-parameter parabolic Mohr criterion could be expressed by principal stresses as

$$\left(\frac{\sigma_1 - \sigma_3}{2}\right)^2 = \lambda\left(\frac{\sigma_1 + \sigma_3}{2}\right) + \lambda\sigma_t - \frac{\lambda^2}{4}. \tag{7}$$

Rewrite with the spherical stress P and the deviatoric stress S:

$$S^2 = \lambda P + \lambda\sigma_t - \frac{\lambda^2}{4}. \tag{8}$$

While transforming the yield criterion from (P, S) coordinate system to (σ, τ) coordinate system, we get

$$\begin{cases} \tan\varphi = \dfrac{d\tau}{d\sigma}, \\ \csc\varphi = \dfrac{dP}{dS}. \end{cases} \tag{9}$$

Consequently, the increment of deviator stress ΔS in the overlapping area can be denoted as

$$\Delta S = \frac{\lambda}{2S}\Delta P. \tag{10}$$

According to the principle of stress superposition, the synthetic hydrostatic stress component is the algebraic sum of the hydrostatic stress of each stress column, and the synthetic deviatoric stress component is the vector sum of the deviatoric stress of each stress column. By combining

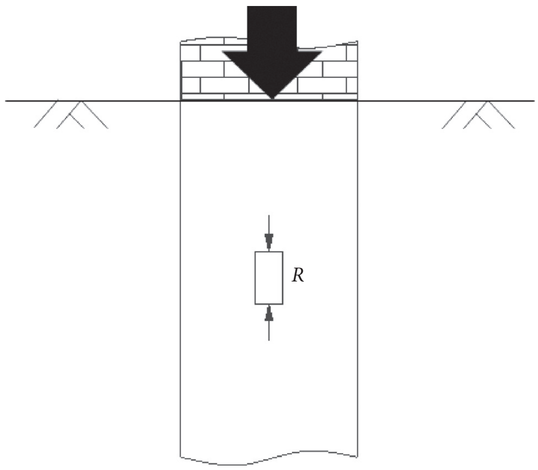

Figure 3: A single stress column.

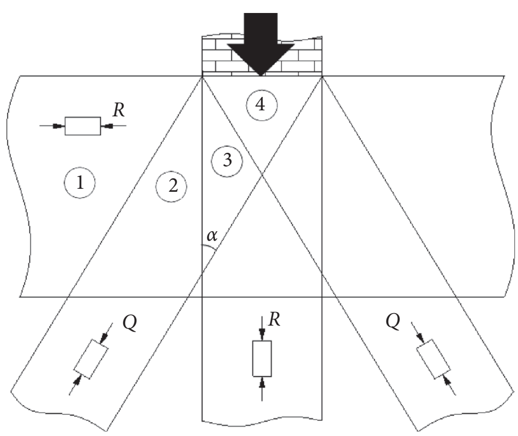

Figure 4: The stress field constructed by 3 stress columns.

with Figure 5, the hydrostatic stress and the deviatoric stress of each stress superimposition area ①~④ in Figure 4 could be calculated as follows:

$$S_1 = \frac{R}{2} = \frac{\sigma_c}{2}, \tag{11}$$

$$S_2 = S_1 + \Delta S = \frac{R}{2} + \frac{\lambda Q}{2R}, \tag{12}$$

$$S_3 = S_2 + \Delta S = \frac{R}{2} + \frac{\lambda Q}{2R} + \frac{\lambda R^2}{2\left(R^2 + \lambda Q\right)}. \tag{13}$$

Apply the cosine theorem in ΔOAB:

$$Q = \frac{2R^3 \cos 2\alpha + 2\lambda R^2}{R^2 - \lambda^2}. \tag{14}$$

In Figure 5,

$$S_3 = \frac{Q}{2}. \tag{15}$$

Combining equations (13), (14), and (15), we get

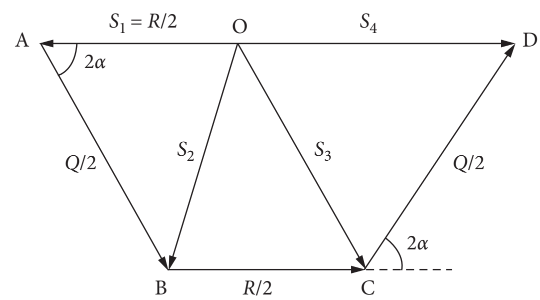

Figure 5: The stress superposition diagram of 3 stress columns.

$$\cos 2\alpha = \frac{(\lambda + R)\cdot\sqrt{-4\lambda^3 R + 4\lambda^2 R^2 + R^4} - R^3 + \lambda R^2 - 2\lambda^2 R}{4\lambda R^2}, \tag{16}$$

$$Q = \frac{\lambda R^3 + 2\lambda^2 R^2 - R^4 + \left(\lambda R + R^2\right)\cdot\sqrt{-4\lambda^3 R + 4\lambda^2 R^2 + R^4}}{2\lambda\left(R^2 - \lambda^2\right)}. \tag{17}$$

The stress status of area ④ in Figure 4 could be presented by

$$P_4 = \frac{R}{2} + \frac{Q}{2} + \frac{R}{2} + \frac{Q}{2} = Q + R, \tag{18}$$

$$S_4 = \frac{Q}{2}\cos 2\alpha + \frac{R}{2} + \frac{Q}{2}\cos 2\alpha - \frac{R}{2} = Q\cos 2\alpha. \tag{19}$$

Consequently, the lower bound solution of bearing capacity of foundation beneath strip footing with 3 stress columns should be

$$\sigma_z = Q_4 + S_4 = Q + R + Q\cos 2\alpha = R + Q(1 + \cos 2\alpha), \tag{20}$$

in which R, Q, and $\cos 2\alpha$ were aforementioned.

3.3. The Case of Nine Stress Columns.

3.3. The Case of Nine Stress Columns. A more sophisticated static allowable stress field composed of 9 stress columns is shown in Figure 6, in which the plastic deformation zone BAC is divided into 9 stress columns with equal angles ($\Delta\theta$). The stress columns suffer from axial compression Q_1, $Q_2 \ldots\ldots$, Q_9, which are determined by parabolic Mohr criterion. Also, a horizontal stress column is affiliated in order not to violate the yield law. For the foundation to the left of stress columns, $\sigma_1 = R$ and $\sigma_3 = 0$; for the base area under the strip footing, $\sigma_1 = \sigma_z$ and $\sigma_3 = \sigma_x > 0$. According to the nonlinear strength criterion, $\varphi_1 > \varphi_2$. The superimposed stress field is shown in Figure 7, in which angles between adjacent deviating stress components are $2\Delta\theta$.

3.4. The Case of Numerous Stress Columns. It is clear that $n+1$ stress columns partition the plastic deformation area into n sector regions with an equal angle $\Delta\theta$; consequently,

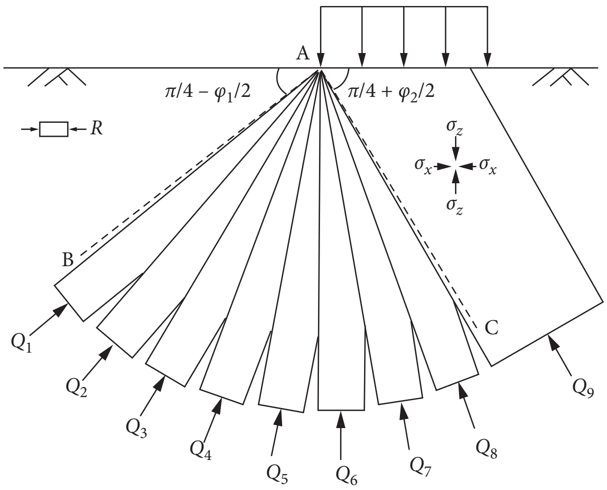

Figure 6: Stress field constructed by 9 stress columns.

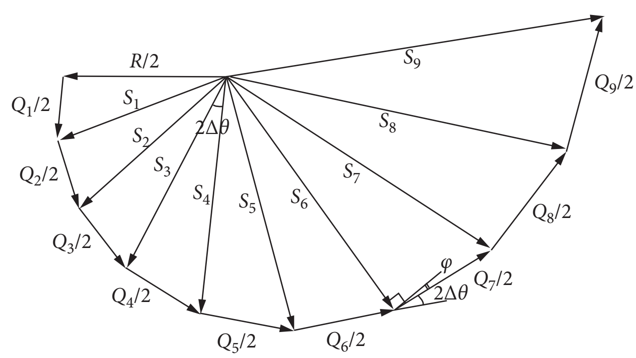

Figure 7: Stress superposition diagram of 9 stress columns.

$$\Delta\theta = \frac{\theta}{n} = \frac{90^\circ + (\varphi_1/2) - (\varphi_2/2)}{n}. \tag{21}$$

And the deviatoric stresses are

$$S_2 = S_1 + \frac{S_1 \cdot 2\Delta\theta}{\cos\varphi} \cdot \frac{\lambda}{2S_1} = S_1 + \frac{2S_1\lambda\Delta\theta}{\sqrt{4S_1^{\ 2} - \lambda^2}}, \tag{22}$$

$$S_3 = S_2 + \frac{S_2 \cdot 2\Delta\theta}{\cos\varphi} \cdot \frac{\lambda}{2S_2} = S_2 + \frac{2S_2\lambda\Delta\theta}{\sqrt{4S_2^{\ 2} - \lambda^2}}, \tag{23}$$

$$S_{n+1} = S_n + \frac{S_n \cdot 2\Delta\theta}{\cos\varphi} \cdot \frac{\lambda}{2S_n} = S_n + \frac{2S_n\lambda\Delta\theta}{\sqrt{4S_n^{\ 2} - \lambda^2}}. \tag{24}$$

The hydrostatic stresses could be given by

$$P_2 = P_1 + \frac{Q_2}{2} = P_1 + \frac{4S_1^{\ 2}\Delta\theta}{\sqrt{4S_1^{\ 2} - \lambda^2}}, \tag{25}$$

$$P_3 = P_2 + \frac{Q_3}{2} = P_2 + \frac{4S_2^{\ 2}\Delta\theta}{\sqrt{4S_2^{\ 2} - \lambda^2}}, \tag{26}$$

$$P_{n+1} = P_n + \frac{Q_{n+1}}{2} = P_n + \frac{4S_n^2\Delta\theta}{\sqrt{4S_n^2 - \lambda^2}}. \tag{27}$$

It should be noted that when the material complies with the nonlinear failure criterion, the angle between the velocity vector and the deviatoric stress vector equals φ. When n increases infinitely, S_1 and P_1 will both approach $R/2$ [1]. Therefore, the lower bound of the foundation bearing capacity should be

$$\sigma_z = \lim_{n\longrightarrow\infty} (Q_{n+1} + S_{n+1}). \tag{28}$$

The solving procedure is shown in Figure 8.

4. Parametric Analysis

4.1. Effect of Stress Column Amount $(n+1)$ on the Lower Bound Solution. Figure 9 shows the relation curve between the number of stress columns and the lower bound solution of bearing capacity with the hypothesis of $\sigma_c = 10$ MPa and $\sigma_t = 1$ MPa. It can be seen that the lower bound solution of bearing capacity gradually is enhanced and converges as the stress column amount increases, which means a better lower bound solution can be obtained by constructing a more precise static allowable stress field. However, the improvement of lower bound solution might be inefficient and meaningless if the stress column number is large enough. For instance, the lower bound bearing capacities are 56.90 MPa and 57.03 MPa, corresponding to $n = 100$ and $n = 10000$, respectively. The relative error between them is only 0.24%.

Referring to Figure 4, the stress distribution in superposition areas with the number of stress columns varying from 11 to 10001 is given in Figure 10, in which P_{101} denotes the hydrostatic stresses of superposition areas within the whole stress field composed of 101 stress columns and S_{1001} represents the deviatoric stresses of superposition areas within the whole stress field composed of 1001 stress columns and so on. It shows that although the amount of stress columns changes significantly, the variation regularity of both hydrostatic and deviatoric stress components is quite similar. The stresses of the superimposition area show a reduction with the improvement of stress field; on the other hand, the superposed stresses elevate ever faster with the increase of the stress column amount it contains. Furthermore, the stress state of all superimposition areas does not violate the aforementioned yield criterion.

4.2. Effect of λ and σ_t/σ_c on the Lower Bound Solution. According to equation (1), the material performance parameter λ could be calculated by the compressive and tensile strength. That is, λ is totally determined by σ_t/σ_c once the compressive or tensile strength is specified. Figure 11 shows the relationship between λ and the lower bound solution of foundation bearing capacity (σ_z) with $\sigma_t/\sigma_c = 0.10$. Intuitively, the lower bound solution is positively correlated with λ. With the enhancement of compressive strength, the

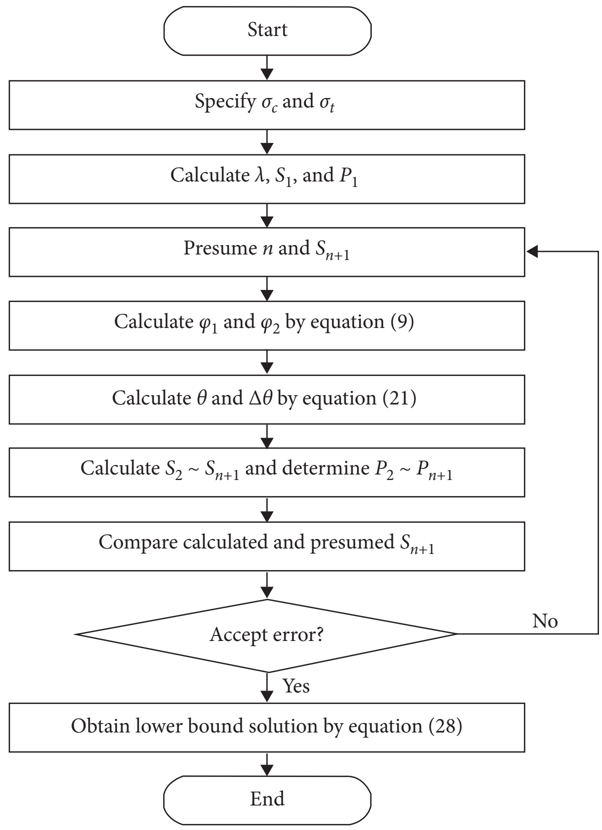

FIGURE 8: Solving flow.

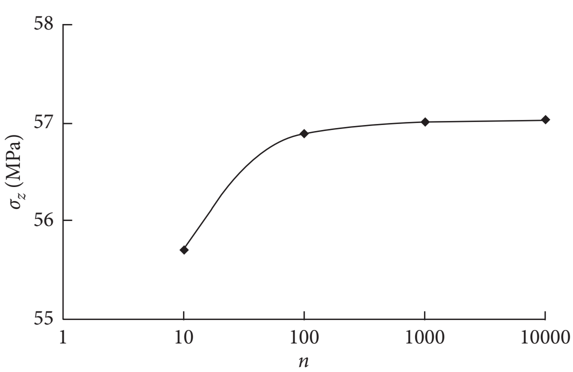

FIGURE 9: Correlation between bearing capacity and stress column amount.

influence of λ on the lower bound bearing capacity will be reduced to some extent. The σ_z~σ_t/σ_c curve is plotted in Figure 12, which proves that when σ_t/σ_c grows up from 1 : 25 to 1 : 5, the lower bound bearing capacity decreases by about 30%. Therefore, σ_t/σ_c has a moderate influence on the lower bound bearing capacity.

5. Verification

Comparative study on uniaxial compression and load test of soft rock foundation in Changsha was performed by Peng et al. [25, 26] and some experimental results are given in

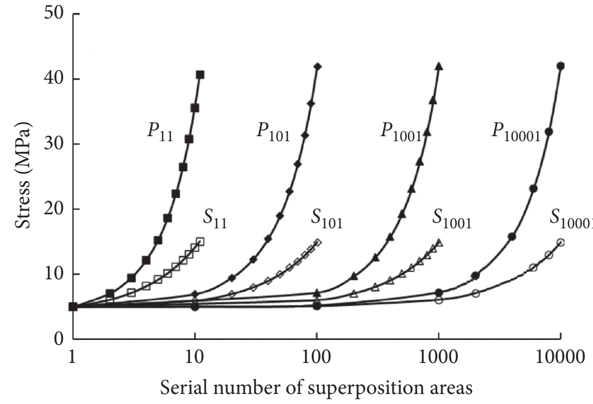

FIGURE 10: Stress distribution in superposition areas.

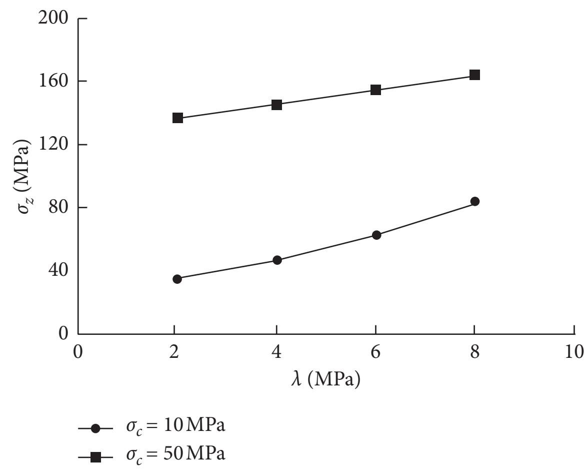

FIGURE 11: Correlation between bearing capacity and λ.

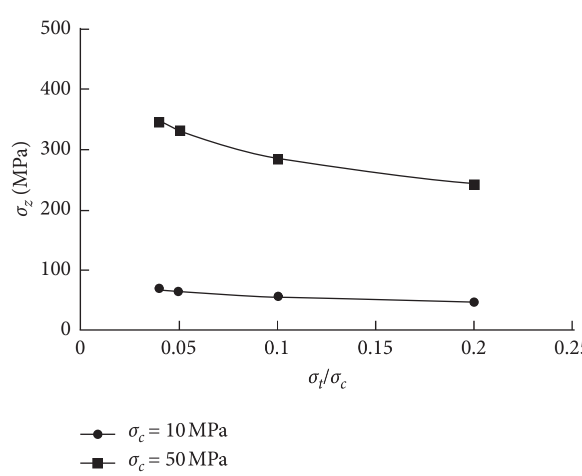

FIGURE 12: Correlation between bearing capacity and σ_t/σ_c.

Table 1, as well as the lower bound solutions. P_L represents the test data of ultimate bearing capacity, f_a is the characteristic value of foundation bearing capacity, and P_c stands for the lower bound solution. Interval strengths are adopted

Table 1: Verification of rock foundation loading tests.

Site	σ_c (MPa)	P_L (MPa)	f_a (MPa)	f_a/σ_c	Pc (MPa)
International Finance Square	2.54	13.59	2.63	1.03	12.25~16.85
Provincial Electromechanical Warehouse	1.99	10.70	3.50	1.76	9.59~13.20
Provincial People's Bank	1.95	11.05	3.00	1.54	9.40~12.93

Table 2: Recommended values of the reduction factor ψ_r.

Integrity of rock foundation	Good	Moderate	Bad
ψ_r	0.5	0.2~0.5	0.1~0.2

since the tensile strength was not clarified in original research, and σ_t is supposed to vary in the range of $0.04\sigma_c$~$0.20\sigma_c$.

By adopting a reasonable stress field, the upper or lower bound solution would be very close to the exact result of the problem. Moreover, the reliability of the proposed solution was validated for the consistency of lower bound bearing capacities and the load tests. The errors might be caused by the following: (1) there exists a size effect in the compressive or tensile strength test, the rock sample cannot represent the entire foundation, and the anisotropy of the rock mass, such as joints, cracks, or weathering degree, could also affect loading test results; (2) during load tests, the failure often occurs in the shallow layer with a depth of 1 ~ 2 times the side length or diameter of the bearing plate; thus, it is difficult to reflect the stress state of deep mass.

Limited by the loading capacity of test devices, it is often difficult to achieve the limit state in load test of rock foundation. Instead, the loading process stops once the load level is no less than 2 times the design requirement of the foundation. Subsequently, 1/3 of the minor value among the proportional limit load and the ultimate load is taken as the characteristic bearing capacity of the rock foundation. Since the theoretical solution is not restricted by the practical working conditions, the characteristic bearing capacity of foundations obtained by this method will not be lower than the test result. Besides, the characteristic value of the bearing capacity of rock foundation can be evaluated by the uniaxial compressive strength of saturated samples in lab (f_{rk}) [27]:

$$f_a = \psi_r \cdot f_{rk}, \tag{29}$$

where ψ_r is the reduction factor and the recommended values are listed in Table 2. It indicates that the recommended characteristic bearing capacity would be always less than half of the uniaxial compressive strength of natural samples and also much smaller than the load test results in Table 1 (1.03~1.76).

6. Conclusion

(1) Stress columns were utilized to construct the static allowable stress field of the foundation beneath strip footing, and the lower bound solution of the foundation bearing capacity based on the two-parameter parabolic Mohr yield criterion is obtained.

(2) The proposed solution is verified by comparison with the load test, which enriches the research results of lower bound analysis in the field of foundation bearing capacity. Moreover, it provides a reference for the lower bound problems subject to nonlinear failure criterion.

(3) The research shows that the characteristic foundation bearing capacity adopted by practical engineering is too conservative, and the bearing capacity of rock foundations has not been fully considered and utilized.

Data Availability

Part of the raw data cannot be shared at this time as the data also form part of an ongoing study.

Conflicts of Interest

The authors declare that there are no conflicts of interest regarding the publication of this paper.

Acknowledgments

This work was funded by Natural Science Foundation, China, Grant no. 51408059.

References

[1] W. F. Chen, *Limit Analysis and Soil Plasticity*, Elsevier Science, Amsterdam, Netherlands, 1975.

[2] S. W. Sloan, "Lower bound limit analysis using finite elements and linear programming," *International Journal for Numerical and Analytical Methods in Geomechanics*, vol. 12, no. 1, pp. 61–77, 1988.

[3] V. L. Andrei, *Three-dimensional Lower Bound Limit Analysis Using Nonlinear Programming*, University of Newcastle, Callaghan, Australia, 1999.

[4] L. Li and B. C. Liu, "Lower bound limit analysis on bearing capacity of slope and its reliability," *Chinese Journal of Rock Mechanics and Engineering*, vol. 20, no. 4, pp. 508–513, 2001.

[5] Q. Y. Zhang, M. T. Luan, and S. F. Zhao, "Lower bound limit analysis of bearing capacity of strip footing due to combined loading," *Journal of China University of Mining & Technology*, vol. 37, no. 3, pp. 364–368, 2008.

[6] S. A. F. Murrell, "The effect of triaxial stress systems on the strength of rocks at atmospheric temperatures," *Geophysical Journal International*, vol. 10, no. 3, pp. 231–281, 1965.

[7] D. Mello, "Reflections on design decisions of practical significance to embankment dams: 17th Rankine lecture," *Géotechnique*, vol. 27, no. 3, pp. 281–355, 1977.

[8] J. Perry, "A technique for defining non-linear shear strength envelopes, and their incorporation in a slope stability method of analysis," *Quarterly Journal of Engineering Geology and Hydrogeology*, vol. 27, no. 3, pp. 231–241, 1994.

[9] J. M. Duncan, P. M. Byrne, K. S. Wong, and P. Mabry, *Strength, Stress-Strain and Bulk Modulus Parameters for Finite Element Analyses of Stresses and Movements in Soil Masses*, University of California, Berkeley, CA, USA, 1980.

[10] SL 274-2001, *Design Specification for Rolled Earth-Rock Fill Dams*, Continuing Education and Development, Inc., Stony Point, NY, USA, 2001.

[11] X. J. Zhang and W. F. Chen, "Stability analysis of slopes with general nonlinear failure criterion," *International Journal for Numerical and Analytical Methods in Geomechanics*, vol. 11, no. 1, pp. 33–50, 1987.

[12] Y. J. Sun, E. X. Song, and J. Yang, "Finite element analysis of earth structure stability with general nonlinear failure criterion," *Engineering Mechanics*, vol. 33, no. 7, pp. 84–91, 2016.

[13] X. C. Shi, Y. F. Meng, and G. Li, "Comparative analyses of several rock strength criteria," *Rock and Soil Mechanics*, vol. 32, no. S1, pp. 209–216, 2011.

[14] Z. M. Cai and W. L. Xu, "The limit loading of slopes for nonlinear Mohr-Coulomb material," *Acta Mechanica Soilda Sinica*, vol. 16, no. 3, pp. 254–258, 1995.

[15] Y. S. Fu, "Comparison of five conventional triaxial strength criteria," *Mining Technology*, vol. 12, no. 3, pp. 74–78, 2012.

[16] L. X. Xiong and L. J. Yu, "Comparative study of three Mohr strength criteria," *Journal of Yangtze River Scientific Research Institute*, vol. 33, no. 4, pp. 81–85, 2016.

[17] X. Ye, S. Wang, S. Zhang, X. Xiao, and F. Xu, "The compaction effect on the performance of a compaction-grouted soil nail in sand," *Acta Geotechnica*, vol. 15, no. 10, pp. 2983–2995, 2020.

[18] X. Y. Ye, S. Y. Wang, Q. Li, and S. Zhang, "Negative effect of installation on performance of a compaction-grouted soil nail in poorly graded stockton beach sand," *Journal of Geotechnical and Geoenvironmental Engineering*, vol. 146, no. 8, Article ID 04020061, 2020.

[19] W. Fang, J. Wang, W. D. X. Zhang, and L. J. Shi, "Lower-bound solution of foundation bearing capacity under circular uniformly distributed load," *Advances in Civil Engineering*, vol. 2020, Article ID 8890450, 6 pages, 2020.

[20] P. N. Zhao, "Stress and displacement of adjacent rock of tunnel under two-parameter parabolic form," *Nonferrous Metal*, vol. 1, pp. 41–44, 1979.

[21] C. X. She and J. Liu, "Two-parameter parabolic-type yield criterion based on mohr strength theory," *Engineering Journal of Wuhan University*, vol. 41, no. 1, pp. 33–36, 2008.

[22] S. Q. Li, X. Y. Jiao, and F. Wang, "Study on conic for mohr curve," *Journal of Liaoning Technical University*, vol. 24, no. 6, pp. 853–855, 2005.

[23] C. G. Li, H. Zheng, and X. R. Ge, "Research on two-parameter parabolic mohr strength criterion and its damage regularity," *Chinese Journal of Rock Mechanics and Engineering*, vol. 24, no. 24, pp. 4428–4433, 2005.

[24] Y. H. Zhu and Q. Fan, "Research on two-parameter parabolic Mohr strength criterion," *Journal of Xi'an University of Science and Technology*, vol. 33, no. 2, pp. 244–248, 2013.

[25] B. X. Peng, F. Jin, and X. H. Wang, "Experimental study on bearing capacity of soft rock of Changsha International Finance Centre," *Chinese Journal of Geotechnical Engineering*, vol. 39, no. s1, pp. 156–160, 2017.

[26] B. X. Peng and X. H. Wang, "Comparative study on PMT and uniaxial compressive test on soft rock," *Rock and Soil Mechanics*, vol. 27, no. 3, pp. 451–454, 2006.

[27] GB 50007-2011, "Code for design of building foundation," 2011.